Silver nanoparticles deposited on calcium hydrogenphosphate – silver phosphate matrix; biological activity of the composite

K. Szmuc[1,5], M. Kus-Liskiewicz[2], Ł. Szyller[1], D. Szmuc[5], M. Stompor[3,5], I. Zawlik[3,5], T. Ruman[4], S. Wołowiec[3,5*], J. Cebulski[1,5]

[1]University of Rzeszów, Faculty of Mathematics and Natural Sciences, 16c Rejtana Ave., 35-959 Rzeszów, Poland
[2]University of Rzeszów, Faculty of Biotechnology, 16c Rejtana Ave., 35-959 Rzeszów, Poland
[3]University of Rzeszów, Faculty of Medicine, 16c Rejtana Ave., 35-959 Rzeszów, Poland
[4]Rzeszów University of Technology, Faculty of Chemistry, 6 Powstańców Warszawy Ave. 35-959 Rzeszów, Poland
[5]FOLPAK, Sp. z o.o. 36-060 Głogów Małopolski, Poland
*Corresponding author: e-mail: swolowiec@ur.edu.pl

The composite containing nanosilver uniformly deposited on matrix composed of $CaHPO_4$ x $2H_2O$ (brushite, *ca* 89 mass %), $CaHPO_4$ (monteonite, *ca* 9.5 mass%), and Ag_3PO_4 (0.5 mas%) was obtained by addition of calcium nitrate and silver nitrate aqueous solution at 30:1 Ca:Ag molar ratio into excess of $(NH_4)_2PO_4$ solution at pH 5.0 – 5.5. The isolated solid was characterized by STEM, XRD, and LDI mass spectrometry. It has been found that nanosilver was uniformly distributed within composite as <10 nm diameter sized nanoparticles. Determination of silver by AAS showed that 60% of silver is present as Ag(0) nanoparticles, the present as matrix Ag_3PO_4 as identified by XRD method. The composite showed strong growth inhibition in *E. coli* and *P. aeruginosa* strains, and moderate towards *S. aureus*. The *C. albicans* cells were the most resistant to the tested material, although still composite was moderately cytostatic for the yeast.

Keywords: silver nanoparticles, composite, calcium hydrogenphosphate matrix, electron microscopy, mass spectrometry.

INTRODUCTION

Silver is known antimicrobial agent[1]. It has been demonstrated that effects on cells and microbes are primarily due to a low level of silver ion release from the nanoparticle surface[2]. Silver(I) ions show high affinity to sulphur donor ligands, which are ubiquitous in lively specimens as cysteine, glutathione, biotin and proteins. Some of the chemical species were isolated and characterized structurally[3–5]. Release of silver(0) and its oxidation is dependent on heterogenic reactions between metal surface and ligands in aqueous surrounding. Therefore high dispersion on silver into nano-size particles favours the reactivity of silver (0/I). Simultaneously, AgNPs could affect some proteins and phosphate lipids and induce collapse of membrane, resulting in cell decomposition and death eventually[1, 2].

Silver nanoparticles (AgNPs) are nowadays commercially available[6]. AgNPs can be obtained from silver(I) salt aqueous solutions by chemical, electrochemical, or photochemical reduction[7]. The colloids of AgNPs dispersed in water are coloured depending on size of AgNP: yellow (10–14 nm), violet (35–50 nm) and grey (60–80 nm)[8]. However, they associate within minutes if no colloid stabilizing agent is present in water. Therefore AgNPs are usually obtained in presence of surfactants[9, 10], immobilized on supporting organic polymers[11–14], or inorganic supports[15–18].

Silver is a noble element with standard electrode potential +0.8 V for Ag(I) reduction. Therefore, no strong reductants are needed to obtain nano-size dispersed silver(0). There are many methods to obtain AgNPs using reductants like BH_4^- [8, 10, 11], or ascorbate and citrate when large scale synthesis is required[7]. It has been demonstrated that not only the propanal[19], but even dimethylformamide[20], and anionic surfactant: sodium bis(2-ethylhexyl)sulfosuccinate (or ethanol used as solvent)

were efficient reductants[9]. Also the silver(I) reduction occur upon sunlight irradiation of the salt solution, especially when other light-sensitive ligands are involved. In fact silver reduction in presence of day light occurs in presence of heparin[12], starch[7], or undefined reductants present in extract of *Ocimum sanctum* leaf[21]. Colloidal silver nanoparticles grow upon reduction by radicals or excited molecules formed in polyvinylpyrrolidone (PVP) in water with isopropanol upon γ-irradiation[13]. Further, AgNPs were deposited on hydroxyapatite or calcium phosphate by combinatorial pulsed laser irradiation in order to fabricate the coating of potential medical applications[22]. Currently the method of laser patterning of calcium phosphate scaffolds with nano silver for bone graft application is on agenda[23].

We have aimed at obtaining silver nanoparticles (AgNP) incorporated in calcium phosphate. Such material has potential application as catalytic silver or antimicrobial layer if deposited on another support. In both cases the active surface of silver must be maximized for efficient activity. Metal silver, as bulk, thin layers or nanoparticles deposit as face centred cubic space groups (Fm_3m, with lattice constant 408.53 pm) with density 10.49 g/cm³ [24]. The active surface of Ag depends on size of AgNP; the parameter usually used is the surface area per gram of silver. There are many methods to obtain nanoparticles of silver(0) dispersed on organic support and inorganic matrices, like calcium phosphate (mostly $Ca_3(PO_4)_2$, called tricalcium phosphate, TCP) or hydroxyapatite[16, 25]. In both cases the AgNPs were obtained from silver(I) nitrate, while the substrates for inorganic matrix were diammonium phosphate and calcium nitrate. The formation of product was pH dependent, therefore the ammonia was used to maintain the pH at about 9[16]. We have partially adopted the conditions of rapid precipitation of silver-doped calcium phosphate described

before[16] except avoiding alkalization of solution with ammonia. Generally we aimed at obtaining the fine composite of nano silver exposed on its surface in order to apply the finely powdered composite as antibacterial and antifungal material.

EXPERIMENTAL

Syntheses and workup of composites

Aqueous solution of 21.0 mM $Ca(NO_3)_2$ and 0.70 mM $Ag(NO_3)$ (20 dm^3) was added dropwise into 21 dm^3 aqueous solution of 20.5 mM $(NH_4)_2HPO_4$. The mixture was stirred mechanically. The 5.5 pH was maintained by addition of phosphoric acid or ammonia. Then, the precipitate was allowed to sediment overnight, part of water solution containing ammonium and nitrate ions was removed and the remaining slurry was filtered upon reduced pressure, washed with copious amount of water until no nitrate, phosphate, or ammonium ions were detected. The wet solid was then dried at 70°C under reduced pressure (5 mm Hg) for 37 hours. All wet processes were performed in red light. Yield of dry product (**1**) was 51.2 g (89% related to theoretical 57.35 g of $CaHPO_4$ + Ag_3PO_4). Dried product was then milled for 4 hours in planetary mill at 300 rpm with 40 g of zirconium oxide mill balls (100 μm diameter)[26]. Then the solids were separated on stacked sieves to recover zirconia milling balls and variable fractions of the product were collected on sieves of descending whole diameters: 200 μm (fraction recycled for milling), 100 μm (for milling balls recovery and large composite particles, later this fraction was recycled into another synthesis), 50 μm and 20 μm. The workup of the precipitate (*vide supra*) yielded 46.65 g distributed between particle size as follows: >200 μm – 1.15 g; 50 μm – 18.33; 20 μm – 16.30 g; <20 μm – 10.87 g (81% yield).

Elemental analysis for Ag, Ca, and P by electron microscopy (Qmaps obtained from HDF detector and EDX spectrometer, *vide infra*) averaged for 14 spots [mass%]: O, 56.61; P, 26.55; Ca, 15.91; Ag, 0.93, which corresponds to relative molar contribution as follows (± standard deviation): O, 3.54 (± 0.33); P, 0.86 (± 0.09); Ca, 1.00 (± 0.31); Ag, 0.008 (± 0.004). The molar ratio of elements was: O:P = 4.1; Ca:Ag = 125.0.

AAS determination of total silver [mass%]: 0.9. 60% of this value corresponds to Ag(0) mass percent, which is 0.54 mas% deposited as AgNP in the composite.

In a bulk synthesis (2 kg scale) 1713 g of the product was isolated as fraction of particle size ≤ 20 μm (76.5 % yield of theoretical yield 2237 g calculated for $CaHPO_4$ + Ag_3PO_4). The elemental analysis showed silver percentage 1.0 mass%, 0.6 mass% of which was Ag(0).

In another synthesis performed in 20:1 Ca:Ag molar stoichiometry the isolated product **2** showed considerably higher total silver percentage (2.6 mass%; 58% of this value corresponds to Ag(0)). However detailed examination of nanocomposite by STEM evidenced that silver was partially distributed in rafts sized ≥20 nm in diameter (*vide infra*, Fig. 1).

Physical measurements

Electron microscopy studies: Samples of composite (ca 100 mg) were suspended in ethanol and transferred to copper grids covered with thin carbon film (carbon type B on 200 mesh, PELCO®, TED PELLA, Inc.) and dried on heat plate at 80°C for 10 minutes. The samples were mounted on single-tilt holder in microscope FEI Tecnai Osiris S/TEM. The measurements were performed in STEM mode (scanning transmission electron microscopy) with BF, DF2 and DF4 and HAADF (high-angle annular dark field) detectors with 200 kV. Super EDX detector was used to collect elemental maps for the samples measured in at least 8 spots. The ESPRIT software was used for live quantification. The average final result of elemental mass percentage was calculated taking the account the spotted area (*vide supra*). The standard deviation of the elemental percentage was used to characterize the sample heterogeneity of composite.

XRD: X-ray powder diffraction experiments were performed on Bruker D8 Advance diffractometer.

Laser desorption/ionization mass spectrometry (LDI MS) analysis on AuNPET: Laser desorption/ionization (LDI) time-of-flight (ToF) mass spectrometry experiments were performed using a Bruker Autoflex Speed reflectron time-of-flight mass spectrometer, equipped with a Smart-Beam II laser (352 nm) in 80-2080 *m/z* range. The laser impulse energy was approximately 60−120 μJ, the laser repetition rate 1000 Hz, and the deflection value was set on *m/z* lower than *m/z* 80. The first accelerating voltage was held at 19 kV, and the second ion-source voltage was held at 16.7 kV. The reflector voltages used were 21 kV (first) and 9.55 kV (second). The data was analyzed using the software provided with the Autoflex instrument (FlexAnalysis version 3.3). Mass calibration (cubic calibration) was performed using internal standards (gold ions and clusters from Au^+ to Au_5^+). The sample for LDI MS measurement was prepared as before[27]. Sum of *ca* 3000 scans was collected for each sample.

Elemental analysis for silver: The elemental composition for Ag^+ and Ag(0) content was performed by atomic absorption spectrometry (AAS) using Analytic Jena Model CONTRA 700 instrument. In a reproducible procedure the sample of composite (*ca* 1 g) was soaked in 2M $NH_3(aq)$ for 15 minutes, the solid was filtered off, washed with water, dried, mineralized in excess concentrated nitric acid to obtain 20 ml stock solution. The solution was diluted 10^4 times with concentrated nitric acid and analysed for silver by AAS. The volume of filtrate was reduced to 1 ml, concentrated nitric acid was added (25 ml), and the mixture was boiled for 1 h. The volume of solution was adjusted to 20 ml with nitric acid. Three aliquots of sample were diluted 10^4 times and analysed for silver by AAS. Total silver content was determined as follows: sample of composite (*ca* 1 g) was mineralized in hot concentrated nitric acid, the volume was adjusted to 20 ml and 10^4 times diluted triple samples were analysed for silver by AAS. Total silver and silver(0) percentage were determined in triple for every composite.

Biology

Antimicrobial tests: Nutrient broth (NB) and potato dextrose broth (PDB) or nutrient agar (NA) and potato dextrose agar (PDA) were used for the preparation of

bacterial or yeast cultures suspension or evaluation of the colony forming unit (CFU), respectively. For serial dilutions, the phosphate buffered saline was used. All materials were sterilized prior to use at 121°C for 20 min. Antibacterial activity of the composites were tested against Gram-(+) *Staphylococcus aureus* ATCC 25923 and Gram-(–) *Escherichia coli* PCM 2209 or *Pseudomonas aeruginosa* ATCC 27853 bacteria strains. For antifungal assay, *Candida albicans* ATCC 14053 strain was chosen. All strains were from the collection of the Centre of Applied Biotechnology and Basic Sciences, RU Poland. Strains were maintained in enriched NB and kept at 4°C. Prior to the microbial assay, the $CaHPO_4$ and composite **1** were sterilized for 30 min at 130°C. The antimicrobial activity of these materials was tested by microorganisms incubation in powders suspensions, followed by colony-forming capability test, in time dependent manner. Bacterial cells were inoculated into 10 mL of NB and incubated in aerobic conditions at 37°C for 12–18 h to give a final concentration of ~10^6 cells/mL (CFU – Colony Forming Unit). Bacterial/fungal growth inhibition was tested by adding the 2.75 mL of sterile potassium hydrogen phosphate buffer solution, 30 mg of each powder ($CaHPO_4$, **1**) and 250 μL of *S.* aureus, *E. coli*, *P. aeruginosa* or *C. albicans* cultures. The samples were incubated in a shaker incubator at 37°C and the sampling time for the experiment was 0, 4, 8, 24, 48 and 72 h. After the exposure period of incubations, 0.1 mL aliquots were taken, serially diluted and plated on agar plates. Bacteria colonies were counted and the numbers of CFU/mL were calculated. Each test was repeated three times (n = 3) and the reported results represent their average values.

Genotoxicity assessment of nanocomposites in the Caco-2 cell line using the Comet assay:

The human epithelial colorectal adenocarcinoma (Caco-2) cell line was obtained from the American Type Culture Collection (ATCC, Manassas, VA) and cultivated in Eagle's minimum essential medium (EMEM) at pH 7.4, supplemented with 20% fetal bovine serum (Sigma-Aldrich, St. Louis, MO, USA), 0.1% penicillin-streptomycin solution in a humidified atmosphere (5% CO_2, 95% air, 37°C). Caco-2 cells were seeded into 6-well cell culture plates (Corning) at a density of 1x10^6 cells/well in 1 ml medium and pre-incubated for 48 h before nanocomposites treatment. Sterilized nanocomposite was added (*ca* 1.0 mg) to three separate wells in a 6-well cell culture plates. The next three wells were a control and contained only cells without nanocomposite. Then Caco-2 cells were incubated under standard culture conditions for 72 h. After 72-h incubation, the nanocomposites were removed and the Caco-2 monolayers were washed five times with PBS and then trypsinated. Genotoxicity of the nanocomposites in the Caco-2 cell line was assess by using the Comet assay (SCGE, single-cell gel electrophoresis). Briefly, the Caco-2 cell pellets were suspended in a pre-warmed low melting point 0.5% agarose and spread on conventional microscope slides (pre-coated with 1% normal melting point agarose and dried) and covered with a coverslip. After 10 min at 4°C, the coverslips were removed and slides were placed in lysis solution for 1 h at 4°C. After lysis slides were washed three times with water and placed in electro-

phoresis chamber with electrophoresis buffer (100 mM Tris base, 500 mM NaCl, 1 mM EDTA, 0.2% DMSO; pH = 9.0) and were run at 4°C for 30 min at 12V. After electrophoresis, slides were washed with distilled water and neutralization buffer (50% ethanol, 20 mM Tris-HCl; pH = 7.4) and dipped in 70% ethanol for 5 min. DNA was stained with YOYO-1 dye and examined with a fluorescence microscope IMAGER D2 (Carl Zeiss).

RESULTS AND DISCUSSION

Silver nanoparticles (AgNPs) form spontaneously upon day light reduction of silver(I) phosphate co-precipitated with calcium phosphate matrix. Calcium triphosphate (CTP) is dominating water insoluble salt formed in alkaline conditions upon mixing of soluble phosphate(V) and calcium(II) salts. Therefore the reagents used to obtain NPs deposited or doped into CTP were diammonium phosphate, silver and calcium nitrates and aqueous ammonia to adjust pH to 9[16]. However, in such conditions the PO_4^{3-} anion is not dominating phosphate due to pK_a = 12.6 for HPO_4^{2-}. Moreover, added ammonia results in formation of $Ag(NH_3)_2^+$ complex ion and eventually leads to incorporation of silver into CTP matrix on the level of 1% even if 5 mol% of available metal ions is Ag^+.

On the other hand, solubility of calcium phosphates was studied both experimentally and theoretically for a three component system: $Ca(OH)_2$-H_3PO_4-H_2O[28]. It has been demonstrated that at pH <6 the least soluble calcium phosphate is dicalcium phosphate (both as $CaHPO_4$ and $CaHPO_4$ x 2 H_2O), while in basic solutions both α- and β- CTP are the least soluble, with hydroxyapatite remaining the most insoluble calcium phosphate throughout 4–12 pH range.

We have applied slightly acidic conditions to co-precipitate calcium phosphate and silver phosphate by aqueous solution $Ca(NO_3)_2$ and $AgNO_3$ into aqueous $(NH_4)_2HPO_4$ solution. The pH of reaction mixture was maintained within 5.0–5.5 by addition of phosphoric acid and/or ammonia. Slow precipitation was enabled by dropwise addition of calcium and silver nitrates. The reaction mixture was maintained in red light in order to minimize the photoreduction of silver(I) to silver(0) and uniform co-precipitation of silver(I) and calcium phosphates. The crude product was filtered off, washed with copious amount of water until no ammonium and nitrate were detected in filtrate. Obtained wet solid was further dried under reduced pressure for 37 hours at 70°C, milled in planetary mill with 100 μm diameter ZrO_2 balls, and sieved to obtain main fraction of particles sized below 50 μm. We have aimed at silver-doped calcium phosphate using 30:1 and 20:1 molar ratio of calcium to silver and molar excess of phosphate anion. Isolated two products were analyzed by STEM, XRD, and laser desorption ionization mass spectrometry using AuNPET technique. We have found that the composites **1** and **2** obtained from 30:1 and 20:1 Ca:Ag mixture contained 0.90 and 2.60 mass% of silver, respectively as determined by atomic absorption spectrometry (AAS).

Composite analysis

Both composites were analysed by STEM in order to characterize the homogeneity of the composites, espe-

cially considering silver distribution. The Qmaps of silver are presented at figure 1 for composite **1** and composite **2**. We found that silver was distributed uniformly in **1**, while nanoparticles of silver(0) as large as 15 nm diameter were observed for **2**. For both composites three samples were subjected for STEM analysis and 12–14 spots were used to obtain averaged Ca, O, P, and Ag mass percentage (see Experimental: Synthesis and workup of composites). Nonetheless, the resolution of STEM analysis did not allow to define the average composition of composites, neither to chemically identify the matrix. Therefore powdered **1** and **2** (fraction sieved under 20 μm particle size) were analysed by XRD.

The matrix of composites **1** and **2** was identified by XRD (see assignments at upper spectrum in red presented for **1** in Fig. 2). Based on database the main component of the matrix were identified as calcium hydrophosphate salt (both as dihydrate, called Brushite, with 86.7% fit, and anhydrous Montenite, with 7.8% fit) as well as silver phosphate (1.8% fit). Thus silver is present in the matrix as Ag_3PO_4, additionally to silver(0) deposited on crystal surface, which was not detected in the sample by XRD. Then, composite silver was totally reduced with ascorbic acid and resulting XRD spectrum showed no presence of Ag_3PO_4. Instead week peaks were observed from nanosilver at 2Θ at 38.1 and 44.3 degree (bottom spectrum at Fig. 2). Thus we have named the composites as Ag@CaAgP (corresponding to **1**) and Ag@CaP, the gray product of silver reduction. In order to monitor the possible changes occurring in **1** upon milling we have also recorded the XRD spectrum of **1** before milling step (after drying step). The spectra of **1** before milling and after milling at 300 rpm speed were imposable. We have concluded that workup of composite by vacuum drying at 70°C and milling at 300 rpm with zirconia did not convert the isolated solid. In fact, milling with 600 rpm resulted in partial thermal conversion of matrix calcium hydrogenphosphate dihydrate with formation of catenaphosphates: bis(catena-phosphate) and calcium--hexaphosphate (Troemelite) and reduction of silver(I) resulting in deposition of large metal drafts in isolated solid observed in STEM pictures.

The silver distribution in **2** was not uniform. A dense rafts observed by STEM in **2** (see Fig. 1, lower trace) were nanosized pure silver (97 mass% in Qmap). Silver was distributed uniformly beyond these nanoparticles both in **2** and **1**. To identify silver species we have recorded the LDI MS spectra for **1** and **2**. The large associated particles were also observed in composites precipitated and worked-up in presence of daylight despite of low starting amount of silver nitrate.

Although the colour of composites was light yellow, as is the colour of silver phosphate, the presence of silver nanoparticles was confirmed by Au nanoparticle enhanced target desorption/ionization mass spectrometry (AuN-PET)[27]. The AuNPET spectrum is presented at Fig. 3. This method showed the presence of silver nanoparticles by peaks corresponding to Ag_2^+, Ag_3^+, and $AuAg_2^+$. The peaks from Au^+, $AuCa^+$, $AuAg^+$, Au_2^+ correspond to gold nanoparticles and gold associates with cations present in matrix (calcium and silver). Isotopic patterns of peaks assigned to Ag^+, Ag_2^+, and Ag_3^+ are almost identical compared to the ones presented in published work by

Niziol and co-workers[29], where analogous peaks origin from AgNP, which were deposited on steel target. Thus we have identified the matrix and found that composites contained silver(0), deposited as <5 nm sized AgNPs in **1** and Ag(0) rafts in **2**.

With identified components as AgNPs, Ag_3PO_4, and $CaHPO_4$ by XRD, MS, and EDX in hand we have performed simple chemical analysis for silver in order to fully characterize **1**. Unlike the spectral methods which are based on laser and X-ray beam excitation and do not give averaged value of element percentages, the large scale averaged sample offer exact determination with common analytical method like AAS.

Silver phosphate is well soluble in 2M NH_3(aq), while silver(0) is not reactive in such conditions. Thus we have treated composites with 2 M NH_3(aq), separated silver(I) – free solid and analysed it after mineralization with concentrated nitric acid as well as filtrate. In separate experiment the composite was mineralized with nitric acid and all three samples were analysed by AAS after dilution. In this way we were able to determine silver(0), silver(I), and total silver percentage in **1** and **2**. We have found that silver (0) and silver (I) percentage was 0.90 and 0.54 for **1** and 2.6 and 1.5 mass% for **2** respectively.

Thus for further studies the composite **1** was chosen, the large scale synthesis was performed at 2 kg scale. The analysis of the product showed no significant differences between the composite obtained in large scale in comparison with **1**, although concentrations of substrate solutions were much higher and concentration of ammonium nitrate, the side product of reaction could interfere with precipitation of pure composite, especially at final phase of large scale synthesis (0.875 M NH_4NO_3 at the end).
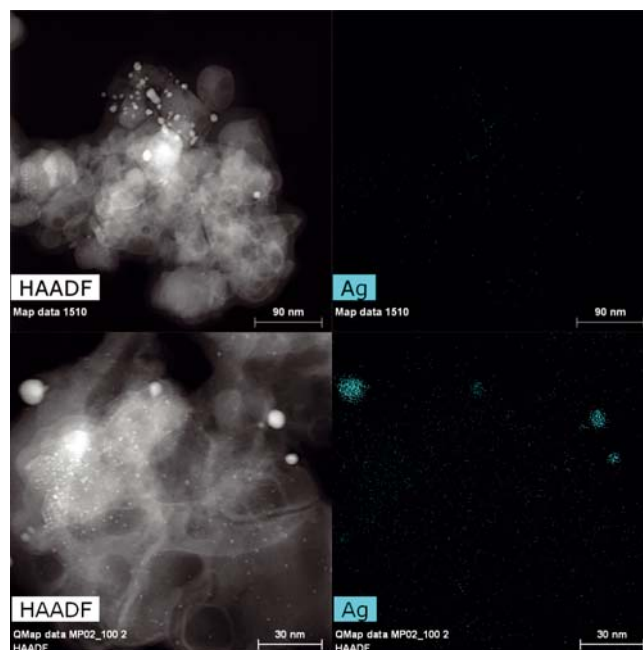

Figure 1. STEM pictures of chosen spot (HAADF) and Qmaps for silver distribution in **1** (upper traces) and **2** (lower traces)
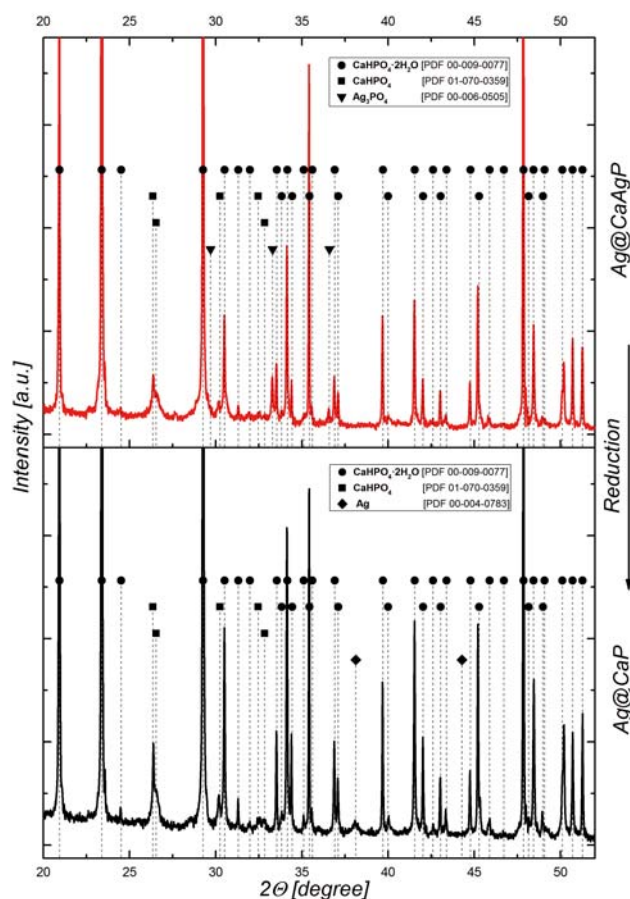
Figure 2. XRD spectra of: **1** (Ag@CaAgP) composite obtained as described in Experimental (upper, in red), and reduced **1** (Ag@CaP) obtained after total reduction of silver(I) into silver(0) with ascorbic acid (bottom, in black).

Ag_3PO_4 in **1** and **2** was 0.46 and 1.1, respectively. The matrix main component was $CaHPO_4$, partially hydrated, depending on the history of synthesis and workup. In case of **1** used further for biologic activity studies the main calcium phosphate was dihydrated form as was shown by XRD.

Silver(0) and silver(I) are known antibacterial agents, especially when silver(0) is dispersed to nano-sized particles. Composite **1** was then tested for toxicity against bacteria and fungi. Gram-positive (*P. aeruginosa*, *S. aureus*) and Gram-negative (*E.coli*) bacteria and yeast (*C. albicans*) were used as the test microorganisms, because they are very common causes of infection in humans and animals[30]. Such organisms are found also, as a food-borne pathogens, usually due to improper food handling[31]. Thus there is a great need for finding new materials with biocidal/fungicidal properties, functioned as a composites for tissue and implant engineering or for food packaging applications. Thus, the antimicrobial effect of the pure matrix ($CaHPO_4$) in comparison with silver-doped composite **1** was examined. Fig. 4 shows the bactericidal and fungicidal efficiency for **1** against *Escherichia coli*, *Staphylococcus aureus*, *Psuedomonas aeruginosa* and *Candida albicans*. Exposure of the silver nanoparticles-incorporated composite (composite **1**) toward tested bacteria and fungi microorganisms, unambiguously resulted in bactericidal or static effect, respectively. For all of the strains, the numbers of colonies were reduced, when organisms have been exposed to **1**, in time- and strain--dependent manner. While, in the control sample (Ct) as well as matrix material ($CaHPO_4$), there is no evidence of growth of inhibition. The *E. coli* and *P. aeruginosa* strains are much more sensitive to **1**, than *S. aureus*. In the first case, the total growth of inhibition was observed
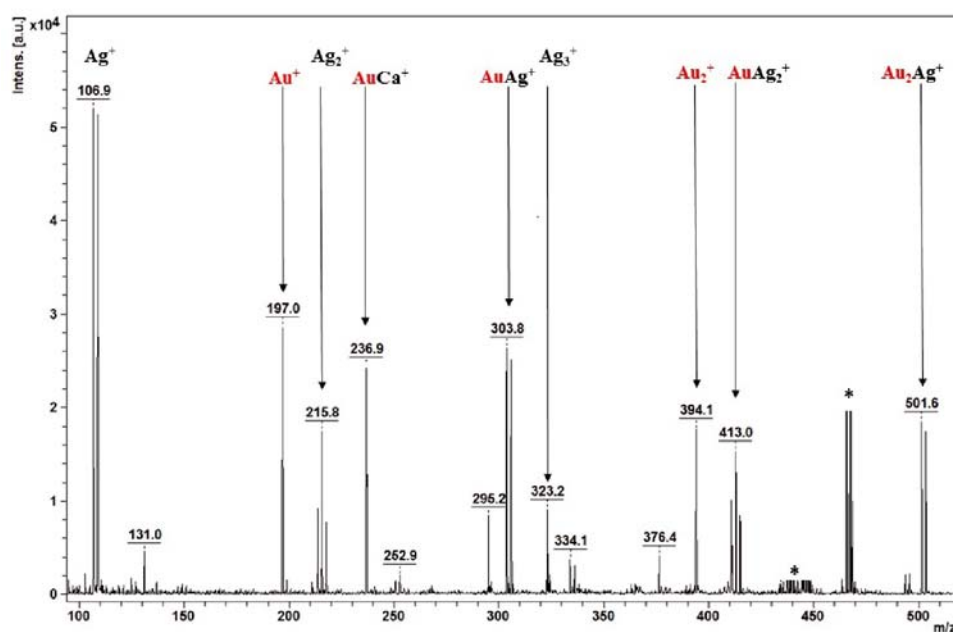
Figure 3. AuNPET mass spectrum of **1** composite. The reference gold⁺ peaks from target are labeled in red. Peaks from organic impurities are labeled with asterisks
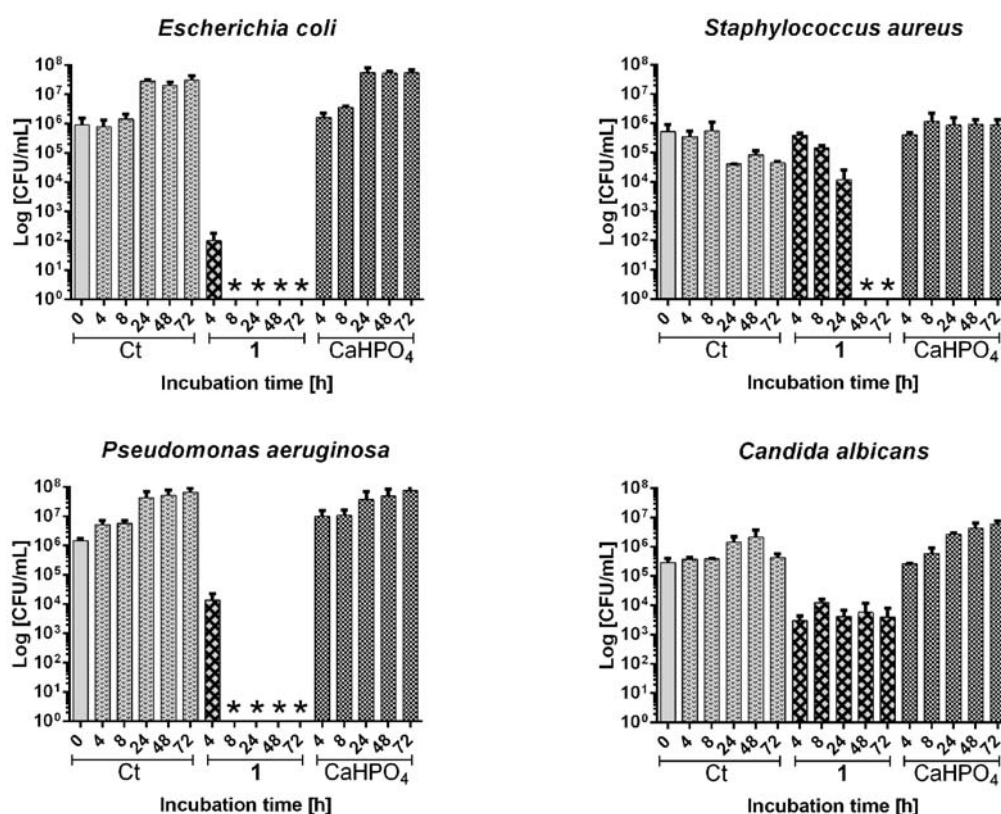
Biological activity of composite 1

Composites comprised silver(0) highly dispersed in inorganic matrix of calcium hydrogenphosphate ($CaHPO_4$) and silver phosphate (Ag_3PO_4). The mass percentage of

after 8 h time of incubation, whereas the bactericidal effect against *Staphylococcus aureus* was achieved after 2 days. The response of the yeast cells indicates that they are the most resistant to the tested material. The silver- incorporated sample has static activity (2–3 logs

reduction) with 72 h time of incubation. Composite **2** showed similar activity in all encountered tests despite of higher percentage of AgNPs.

Composite **1** was also preliminarily tested for biological activity towards mammalian cells. Caco-2 culture was used as fast proliferating model for human digestion system cells. We have found that after 72 hours of incubation of Caco-2 in presence of the viability of cells was below 10%. The cells were isolated and tested for genotoxicity by common comet assay. Caco-2 cells exposed to **1** showed DNA damage. Our results indicated that the noanocomposite had genotoxic effect in the Caco-2 cells. Representative images of comet assay analysis of Caco-2 cells are presented in Fig. 5. It has been already shown that AgNPs were able to affect drastically Caco-2 cells. Villa et al. reported that after the 24 h exposure to 50 μg/mL no viable cells were observed[32]. In our study, we have shown that silver nanoparticles deposited on calcium hydrogenphosphate had genotoxic effect on the Caco-2 cells.

Final remarks

Due to its antimicrobial properties composites like **1** might find the application as antimicrobial agent protecting against bacteria or fungi and therefore can be applied as component in medical clothes or in food packages, for instance as filling for polyethylene (PE) foils. Preliminarily we have found that PE filled with 10% composite **1** did not transfer silver into food upon contact. Moreover, composite **1** releases silver(0) upon long term light exposure and mechanical distortions, which improves the antimicrobial properties of such modified foil.

CONCLUSIONS

Silver(0) deposited in the matrix composed of silver phosphate and calcium hydrogenphosphate can be obtained from calcium nitrate, silver nitrate, and diammonium phosphate by wet method within pH 5.0–5.5. Silver(0) and silver(I) phosphate are uniformly distributed within

Figure 4. Graphs demonstrating viability of bacteria *Escherichia coli*, *Staphypococcus aureus*, and *Pseudomonas aeruginosa* and *Candida albicans* fungi monitored within 72 hours. Ct – control experiment on NA, NB (for bacteria) and PDB, PDA (for fungi) medium, CaHPO4 – the experiment in presence of solid CaHPO$_4$, **1** – the experiment in presence of composite **1**

Figure 5. Representative images of Comet assay analysis of Caco-2 cells; left panel: untreated Caco-2 cells, showing a circular shape indicating absence of DNA damage; right panel: exposed Caco-2 cells, exhibiting a tail, indicating DNA damage

the matrix when molar ratio of calcium to silver is kept at the level 30:1. Almost one mass percent of silver is present in the composite, 60% of which is deposited as <5 nm sized nanoparticles.

Obtained material contains biologically available silver resulting in high antibacterial properties of the composite. Uniform distribution of silver as <5 nm sized nanoparticles in the composite enables to apply this material as antibacterial agent instead of commercially available AgNPs. Replacement of AgNPs by its nanocomposite with calcium hydrogenphosphate provides the possibility to avoid the environment overload with

silver and to reduce the consumption of silver for antimicrobial purposes. It seems particularly important in the context of its genotoxic effect described earlier and confirmed herein.

ACKNOWLEDGEMENTS

LITERATURE CITED

1. Li, W.R., Xie, X.B., Shi, Q.S., Zeng, H.Y., Ou-Yang, Y.S. & Chen, Y.B. (2010).Antibacterial activity and mechanism of silver nanoparticles on Escherichia coli. *Appl. Microbiol. Biotechnol*. 85, 1115–1122. DOI: 10.1007/s00253-009-2159-5.

2. Lubick, N. (2008). Nanosilver toxicity: ions, nanoparticles—or both? *Environ. Sci. Technol*. 42, 8617–8617. DOI: 10.1021/es8026314.

3. Leung, B.O., Jalilehvand, F., Mah, V., Parvez, M. & Wu, Q. (2013). Silver(I) Complex Formation with Cysteine, Penicillamine, and Glutathione. *Inorg. Chem*. 52, 4593–4602. DOI: 10.1021/ic400192c.

4. Aoki, K. & Saenger, W. (1983). Interactions of Biotin with Metal Ions. X-Ray Crystal Structure of the Polymeric Biotin- Silver(I) Nitrate Complex: Metal Bonding to Thioether and Ureido Carbonyl Groups. *J. Inorg. Biochem*. 19, 269–273. DOI: 10.1016/0162-0134(83)85031-4.

5. Panzner, M.J., Bilinovich, S.M., Youngs, W.J. & Leeper, T.C. (2011). Silver metallation of hen egg white lysozyme: X-ray crystal structure and NMR studies. *Chem. Commun*. 47, 12479–12481. DOI: 10.1039/c1cc15908a.

6. Highly dispersed AgNPs (10 nm diameter sized) are available in isopropyl alcohol, aqueous buffered solutions with sodium citrate stabilizer, or in polyvinylpyrrolidone (PVP) coat from worldwide chemicals distributors.

7. Abou El-Nour, K.M.M., Eftaiha, A., Al-Warthan, A., Ammar, R.A.A. (2010). Synthesis and applications of silver nanoparticles. *Arab. J. Chem*. 3, 135–140. DOI: 10.1016/j.arabjc.2010.04.008.

8. Mulfinger, L., Solomon, S.D., Bahadory, M., Jeyarajasingam, A.V., Rutkowsky, S.A., Boritz, C. (2007). Synthesis and Study of Silver Nanoparticles. *J. Chem. Educ*. 84, 322–325. DOI: 10.1021/ed084p322.

9. Liz-Marźan, L. & Lado-Touriňo, I. (1996) Reduction and stabilization of silver nanoparticles in ethanol by nonionic surfactants. *Langmuir*. 12, 35853–3589. DOI: 10.1021/la951501e.

10. Radziuk, D., Skirtach, A., Sukhorukov, G., Shchukin, D. & Mohwald, H. (2007).Stabilization of silver nanoparticles by polyelectrolytes and poly(ethylene glycol). *Macromol. Rapid Commun*. 28, 848–855. DOI: 10.1002/marc.200600895.

11. Malina, D., Sobczak-Kupiec, A., Wzorek, Z. & Kowalski, Z. (2012). Silver nanoparticles with different concentrations of polyvinylpyrrolidone. *Dig. J. Nanomat. Biostruct*.7, 1527–1534.

12. Huang, H. & Yang, X. (2004). Synthesis of polysaccharide-stabilized gold and silver nanoparticles: a green method. *Carbohydr. Res*. 339, 2627–2631. DOI: 10.1016/j.carres.2004.08.005.

13. Shin, H.S., Yang, H.J., Kim, S.B. & Lee, M.S. (2004). Mechanism of growth of colloidal silver nanoparticles stabilized by polyvinyl pyrrolidone in γ-irradiated silver nitrate solution. *J. Colloid Interface Sci*. 274, 89–94. DOI: 10.1016/j.jcis.2004.02.084

14. Hu, Y., Zhao, T., Zhu, P., Liang, X., Sun, R. & Wong, P.C. (2016). Tailoring size and coverage density of silver nanoparticles on monodispersed polymer spheres as highly sensitive SERS substrates. *Chem. Asian J*. 11, 2428–2435. DOI: 10.1002/asia.201600821.

15. Supraja, N., Prasad, N.T.N.V.K.V. & David, E. (2016). Synthesis, characterization and antimicrobial activity of the micro/nano structured biogenic silver doped calcium phosphate. *Appl. Nanosci*. 6, 31–41. DOI: 10.1007/s13204-015-0409-7.

16. Range, S., Hagmeyer, D., Rotan, O., Sokolova, V., Verheyen, J., Siebers, B. & Epple, M. (2015). A continuous method to prepare poorly crystalline silver-doped calcium phosphate ceramic with antibacterial properties. *RSC Adv*. 5, 43172. DOI: 10.1039/C5RA00401B.

17. Shin, Y.S., Park, M., Kim, H.K., Jin, F.L. & Park, S.J. (2014). Synthesis of Silver-doped Silica-complex Nanoparticles for Antibacterial Materials. *Bull. Korean Chem. Soc*. 35, 2979–2984. DOI: 10.5012/bkcs.2014.35.10.2979.

18. Muniz-Miranda, M. (2003). Silver-doped silica colloidal nanoparticles. Characterization and optical measurements. *Colloids Surf. A Physicochem. Eng. Asp*. 217, 185–189. DOI: 10.1016/S0927-7757(02)00575-7.

19. Muzamil, M., Khalid, N., Aziz, M.D. & Abbas, S.A. (2014). Synthesis of silver nanoparticles by silver salt reduction and its characterization. *IOP Conf. Ser: Mater Sci. Eng*. 60, 1–8. DOI: 10.1088/1757-899X/60/1/012034.

20. Pastoriza-Santos, I. & Liz-Marźan, L.M. (1999). Formation and stabilization of silver nanoparticles through reduction by N,N-dimethylformamide. *Langmuir*. 15, 948–951. DOI: 10.1021/la980984u.

21. Bykkam, S., Ahmadipour, M., Narisngam, S., Kalagadda, V.R. & Chidurala, S.C. (2015). Extensive studies on X-ray diffraction of green synthesized silver nanoparticles. *Adv. Nanopart*. 4, 1–10. DOI: 10.4236/anp.2015.41001.

22. Socol, G., Socol, M., Sima, L., Petrescu, S., Enulescu, M., Sima, F., Miroiu, M., Popescu-Pelin, G., Stefan, N., Critescu, R., Mihailescu, C.N., Stanulescu, A., Sutan, C. & Mihailescu, I.N. (2012) Combinatorial pulsed laser deposition of Ag-containing calcium phosphate coatings. *Dig. J. Nanomat. Biostruct.* 7, 563–576.

23. Rau, J., Fosca, M., Graziani, V., Egorov, A.A., Zobkov, Y.V., Fedotov, A.Y., Ortenzi, M., Caminiti, R., Baranchikov, A. & Komlev, V.S. (2016). Silver-doped calcium phosphate bone cements with antibacterial properties. *J. Funct. Biomater*. 7, 10; DOI: 10.3390/jfb7020010.

24. http://periodictable.com/Elements/047/data.html

25. Iconaru, L.S., Chapon, P., LeCoustumer, P. & Predoi, D. (2014). Antimicrobial Activity of Thin Solid Films of Silver Doped Hydroxyapatite Prepared by Sol-Gel Method. *Scientific World J*. 11, 165351. DOI: 10.1155/2014/165351.

26. Hardness of ZrO_2 (zirconia) is considerably higher (1200 kg/mm^2 or 11.8 GPa [26a] in comparison with calcium phosphates (2.7–4.9 GPa);

26a; a: Grave, O.A. (2008). in Chapter 10, pp 169-193. *Ceramic and glass materials. Structures, properties and processing*. James F. Shackelford and Robert H. *Doremus Eds.* Springer Science+Business Media, LLC. DOI: 10.1007/978-0-387-73362-3.

26b: Slósarczyk, A. & Białoskórski, J. (1998). Hardness and fracture toughness of dense calcium–phosphate-based materials. *J. Mat. Sci.: Materials in Medicine*. 9, 103–108.

27. Sekuła, J., Nizioł, J., Rode, W. & Ruman, T.S. (2015). Gold nanoparticle-enhanced target (AuNPET) as universal solution for laser desorption/ionization mass spectrometry analysis and imaging of low molecular weight compounds. *Anal. Chim. Acta*. 875, 61–72. DOI: 10.1016/j.aca.2015.01.046.

28. Chow, L.C. & Eanes, E.D (2001).Solubility of Calcium Phosphates. in Octacalcium Phosphate. *Monogr. Oral Sci*. 13, 94–111. DOI: 10.1159/isbn.978-3-318-00704-6.

29. Nizioł, J., Zieliński, Z., Rode, W. & Ruman, T. (2013). Matrix-free laser desorption-ionization with silver nanoparticle enhanced steel targets, *Int. J. Mass Spectrom*. 335, 22–32. DOI: 10.1016/j.ijms.2012.10.009.

30. Jarvis, W.R. & Martone, W.J. (1992). Predominant pathogens in hospital infections. *J. Antimicrob. Chemother*. 29, 19–24. DOI: 10.1093/jac/29.suppl_A.19.

31. Zhang, X., Gang, X., Wang, Y., Zhao, Y., Su, H. & Tan, T. (2017). Preparation of chitosan-TiO$_2$ composite film with efficient antimicrobial activities under visible light for food packaging applications. *Carbohydr. Polymer*. 169, 101–107. DOI: 10.1016/j.carbpol.2017.03.073.

32. Vila, L., Marcos, R. & Hernández, A. (2017). Long-term effects of silver nanoparticles in Caco-2 cells. *Nanotoxicol*. 11, 771–780. DOI: 10.1080/17435390.2017.1355997.